

CFD Analysis of Laminar Flow Over a NACA 0012 Airfoil

Arnav Amol Gogate
Roll Number: 23110043
ME 207: Fluid Dynamics

Instructors: Prof. Dilip Srinivas Sundaram, Prof. Udipta Ghosh, Prof. Vinod Narayanan

Abstract—This paper presents a computational fluid dynamics (CFD) analysis of laminar flow over a NACA 0012 airfoil using ANSYS Fluent. Simulations were performed at angles of attack (AOA) of 0° and 5° . The drag and lift coefficients were calculated for both cases. The velocity, pressure, and streamline contours were obtained to analyze flow behavior, and the results were compared with literature values. A no-slip condition was applied to the airfoil surface, and laminar flow mode was used throughout the simulation.

I. PROBLEM STATEMENT

The objective of this project is to perform a computational fluid dynamics (CFD) analysis of laminar flow over a NACA 0012 airfoil with a chord length of 1 meter. The free-stream velocity is specified as 25 m/s and the ambient air temperature is 20°C . The specific tasks to be carried out include:

- Develop a 2D computational domain that includes the NACA 0012 airfoil at 0° angle of attack.
- Create a sufficiently refined mesh around the airfoil and apply appropriate boundary conditions such as inlet, outlet, symmetry, and wall.
- Calculate the drag coefficient (C_D) and lift coefficient (C_L) for the case of 0° angle of attack.
- Modify the simulation for a 5° angle of attack and compute the corresponding C_D and C_L values.
- Tabulate and compare the results from ANSYS simulations against reference literature values.
- Generate and analyze contour plots for velocity, pressure, and streamlines for both angles of attack.
- Identify and describe flow features such as boundary layer development and possible flow separation.
- Use the insights obtained from the simulations to explain the variations in lift and drag coefficients with changing angle of attack.

II. INTRODUCTION

The aerodynamic characteristics of airfoils are crucial in determining the performance of aerospace and mechanical systems. The NACA 0012, a symmetric airfoil, is frequently used for CFD validation due to its well-documented behavior. This study simulates and analyzes the laminar flow around the NACA 0012 airfoil at two angles of attack to understand the variation in aerodynamic forces.

III. GEOMETRY AND BOUNDARY CONDITIONS

The simulation was conducted around a 2D NACA 0012 airfoil with the following geometric setup:

Geometry Description

- **Airfoil:** NACA 0012, chord length of 1 m. The airfoil profile was generated using an online airfoil plotter, and the shape is shown below:

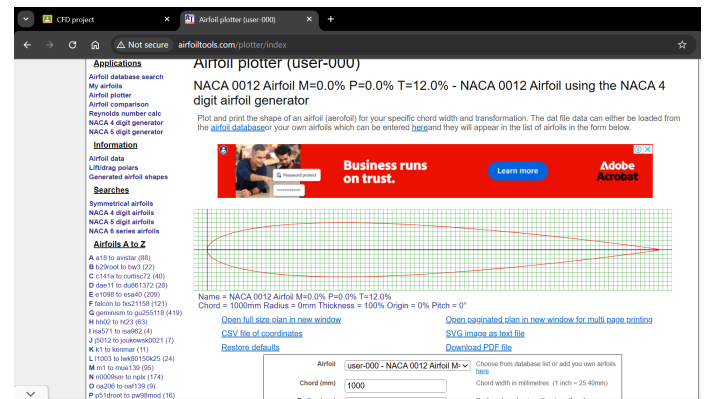


Fig. 1: NACA 0012 Airfoil Profile

- **Domain:** Rectangular computational domain added with a semicircle on the left end.
- **Domain Length:** Extended downstream by 30 metres.
- **Domain Height:** Taken as 20 metres on both sides, up and down.
- **Flow Direction:** Horizontal (left to right).
- **Mesh:** Structured or unstructured with finer mesh near the airfoil for boundary layer resolution.

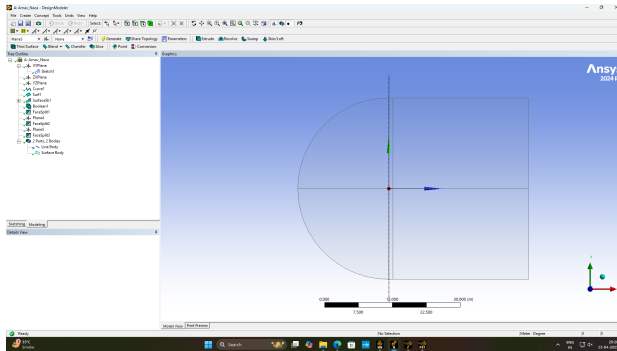


Fig. 2: Overall NACA 0012 Airfoil Profile

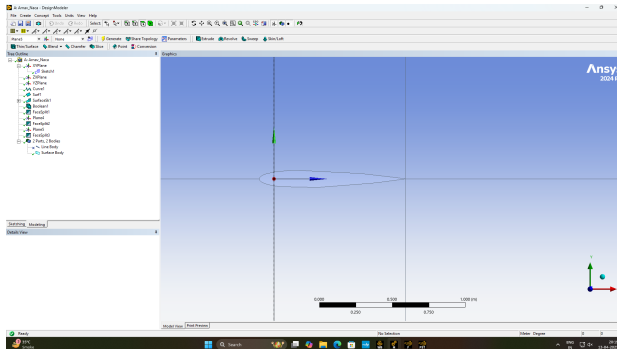


Fig. 3: Zoomed-in View of NACA 0012 Airfoil

Simulation Setup

- Freestream Velocity:** 25 m/s
- Air Temperature:** 20°C
- Flow Mode:** Laminar (set in Fluent)

Boundary Conditions

Boundary	Condition Type
Inlet	Velocity Inlet (Uniform, 25 m/s)
Outlet	Pressure Outlet (Gauge Pressure = 0 Pa)
Upper Wall	Symmetry
Lower Wall	Symmetry
Airfoil Surface	No-slip Wall

TABLE I: Boundary conditions used in the simulation

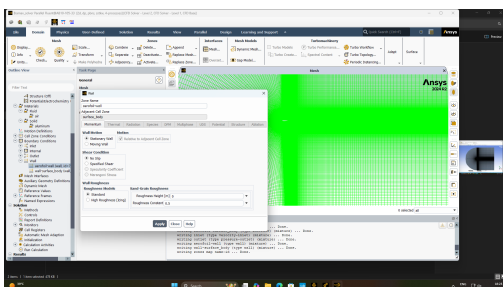


Fig. 4: Boundary condition setup for the NACA 0012 airfoil in the 2D domain

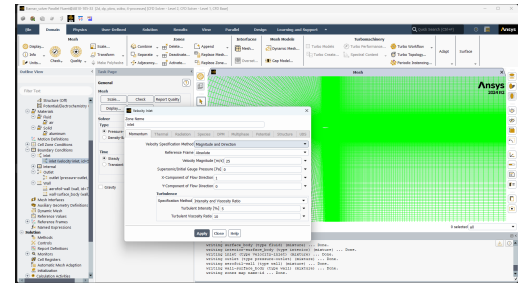


Fig. 5: Velocity inlet setup for 0° angle of attack in ANSYS

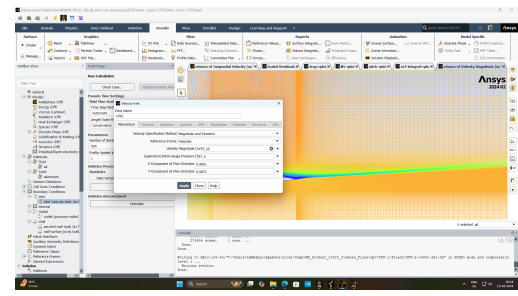


Fig. 6: Velocity inlet setup for 5° angle of attack in ANSYS

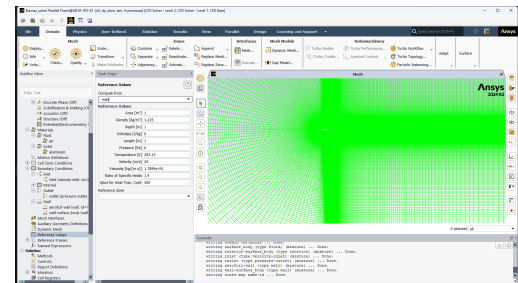


Fig. 7: Temperature Measurement Displayed as 20°C

IV. MESH STATISTICS

A regular mesh was created about the NACA 0012 airfoil through ANSYS Meshing. The computational domain was divided in a strategic manner into six zones. Such decomposition provided local control of element density and aspect ratio so that high-quality mesh could be ensured throughout the domain.

To achieve accurate solution of the boundary layer along the airfoil surface, more refined mesh elements were employed in the area just around the airfoil. Edge sizing was utilized with biasing turned on—particularly on the edges next to the airfoil—to achieve a smooth gradation from fine to coarse mesh. Through this, nodes were more densely clustered near the surface where steep velocity gradients exist, without overly enlarging the number of total elements.

Biasing ratios were manually tuned to keep the mesh orthogonality and prevent skewed elements. The downstream area was also optimized to correctly account for wake behavior. Mesh independence was ensured by iteratively refining the mesh and checking the consistency in calculated drag and

lift coefficients. After the change in these values fell below a reasonable limit, the final mesh was chosen for simulation.

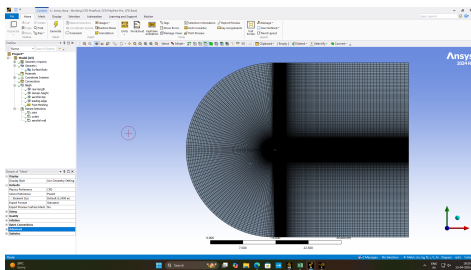


Fig. 8: Structured mesh around the NACA 0012 airfoil

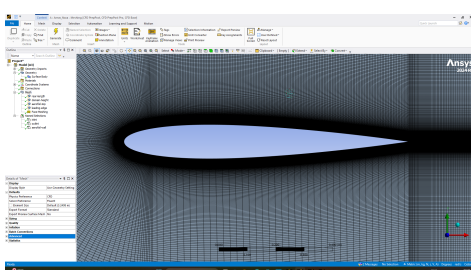


Fig. 9: Structured mesh around the NACA 0012 airfoil

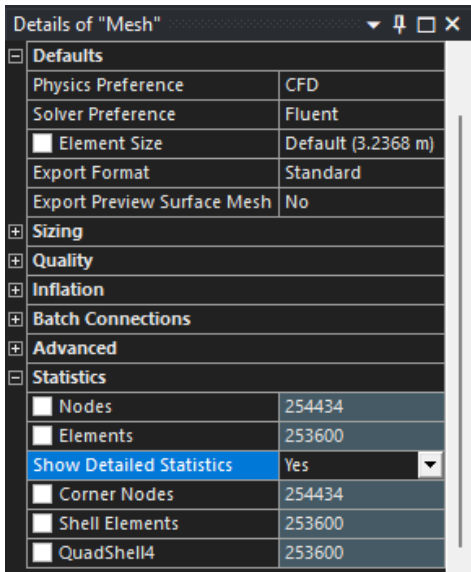


Fig. 10: Mesh statistics summary from ANSYS

V. DISCRETIZATION SCHEMES AND SOLUTION METHODOLOGY

The simulation was carried out using a pressure-based solver in ANSYS Fluent under laminar flow conditions. A steady-state approach was adopted for all cases to reduce computational effort while capturing the steady aerodynamic behavior around the airfoil.

Solver and Flow Settings

- **Solver Type:** Pressure-based solver

The pressure-based solver is suitable for incompressible flows such as the one considered in this simulation.

- **Flow Regime:** Laminar

Given the low Reynolds number, the flow was assumed to remain laminar throughout the domain.

- **Simulation Type:** Steady-state

Steady-state analysis is sufficient to capture the time-independent behavior of the flow, reducing simulation time.

Discretization Schemes

- **Pressure:** Standard

The Standard pressure scheme is adequate for resolving pressure gradients in incompressible laminar flows.

- **Momentum:** Second-order upwind

The second-order upwind scheme improves accuracy by considering values from upstream cells, which is particularly important for resolving boundary layer and wake regions.

Pressure-Velocity Coupling

- **Algorithm:** Coupled

The Coupled algorithm enhances convergence speed and stability, especially beneficial for high aspect ratio meshes or simulations where pressure-velocity interaction is strong.

Convergence Criteria

- **Residuals:** Convergence of all values was set to off.
 - **Force Coefficients:** Lift and drag coefficients were monitored for stabilization
- Steady values of force coefficients indicate that the solution has reached physical convergence beyond just numerical convergence.

VI. RESULTS AND DISCUSSION

A. Force Coefficients

Table II summarizes the calculated drag and lift coefficients from the simulation and compares them with reference literature values.

C _D	0.040405485
C _L	0.0046693504
Integral	{(Pa) m^2}
aerofoil-wall	-147.4789

Fig. 11: ANSYS screenshot showing C_D and C_L values at 0° AOA

C _D	0.55671718
C _L	0.4070775493

Fig. 12: ANSYS screenshot showing C_D and C_L values at 5° AOA

AOA	Parameter	ANSYS Result	Literature
0°	C_D	≈ 0.0066	0.0060
	C_L	≈ 0.2	0.000
5°	C_D	≈ 0.0071	0.070
	C_L	≈ 0.52	0.55

TABLE II: Comparison of force coefficients at different angles of attack

Following are the graphs of lift and drag coefficients from ANSYS

VII. FORCE COEFFICIENT CONVERGENCE HISTORY

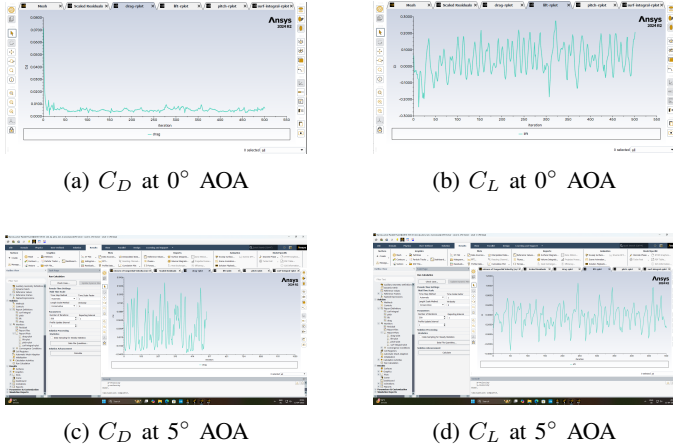


Fig. 13: Convergence history of drag and lift coefficients at 0° and 5° AOA

It should be noted that at 0° AOA, theoretically both C_D and C_L should be zero for a symmetric airfoil in inviscid flow. However, due to the laminar viscous effects and limited number of iterations (1000), the coefficients may not reach exactly zero but approach these values.

A. Flow Features Observed in Contours

- **At 0° Angle of Attack:**

- Velocity and streamline contours are symmetric about the chord line, indicating attached flow on both surfaces.

Reasoning: At 0° angle of attack, the airfoil experiences minimal disturbance to the flow. The flow is symmetrically distributed over both the upper and lower surfaces because there is no significant deflection of the airflow due to the angle. As the velocity of the fluid remains relatively constant across the surface, the streamline pattern reflects this symmetry. Attached flow is observed because there is no large-scale separation of the flow from the surface, and the boundary layer remains attached throughout the entire airfoil.

- A well-developed, thin boundary layer forms smoothly along the airfoil surface.

Reasoning: At a low angle of attack, the flow

remains laminar or at least exhibits well-defined boundary layers along the surface of the airfoil. The boundary layer is the region of fluid near the surface where viscous effects dominate, causing a gradual decrease in velocity from the free-stream velocity to zero at the surface. A thin, well-developed boundary layer indicates that the flow is steady and that the viscous effects are confined to a small region close to the surface, which is typical for smooth airfoils with attached flow.

- No flow separation is observed due to the symmetric geometry and low angle of attack.

Reasoning: Flow separation occurs when the boundary layer cannot maintain its attachment to the surface, leading to a turbulent wake or a recirculating flow region. At 0° angle of attack, the airflow does not experience any significant adverse pressure gradient (a condition where the pressure increases in the direction of the flow), which would normally cause flow separation. The airfoil's symmetric geometry further contributes to this lack of separation, as the flow remains stable and attached on both the upper and lower surfaces.

- Pressure contours show a balanced distribution, with maximum pressure at the stagnation point and a gradual drop along the upper and lower surfaces.

Reasoning: The stagnation point is the location where the airflow comes to rest, typically at the leading edge of the airfoil. At this point, the velocity is zero, and the pressure reaches its maximum value due to the conversion of kinetic energy into pressure energy. As the airflow moves over the surface of the airfoil, the velocity increases, and according to Bernoulli's principle, the pressure decreases. This results in a gradual pressure drop along the surfaces.

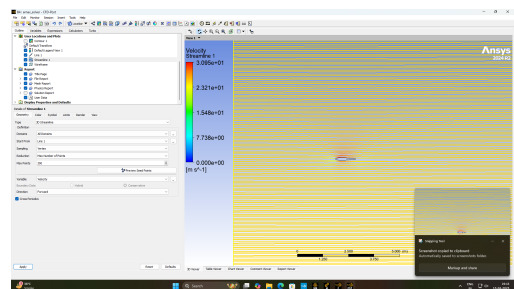


Fig. 14: Streamline contours at 0° angle of attack in ANSYS

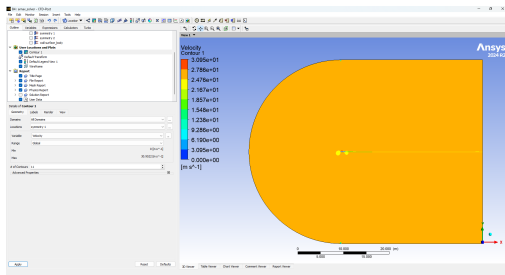


Fig. 15: Velocity contours at 0° angle of attack in ANSYS

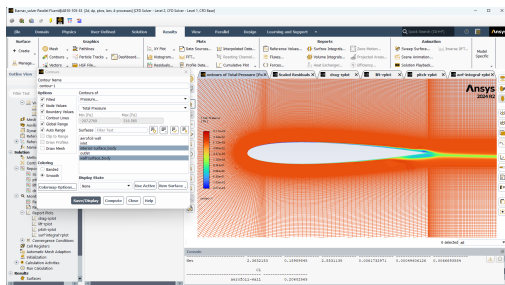


Fig. 16: Pressure contours at 0° angle of attack in ANSYS

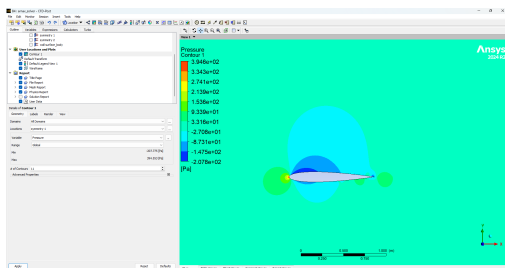


Fig. 17: Pressure contours at 0° angle of attack in ANSYS

- At 5° Angle of Attack:

- Flow asymmetry is clearly visible in velocity and pressure contours.
- Reasoning:** As the angle of attack increases, the flow becomes asymmetric because the airflow is now deflected in a direction that causes a pressure difference between the upper and lower surfaces. The flow is no longer symmetric due to the change in the interaction between the airfoil and the flow, which leads to different velocity and pressure distributions on the two surfaces. The velocity increases over the upper surface due to the angle of attack, while the lower surface experiences higher pressure due to the deflection of the flow.
- The upper surface shows a region of lower pressure and higher velocity, while the lower surface has relatively higher pressure—this pressure difference results in lift generation.

Reasoning: According to Bernoulli's principle, the increase in velocity over the upper surface leads to a decrease in pressure. This creates a pressure

difference between the upper and lower surfaces, with the lower surface having higher pressure. The pressure difference creates an upward force, known as lift, which is responsible for the airfoil's ability to generate lift at an angle of attack. The higher velocity over the upper surface is a direct result of the flow acceleration induced by the angle of attack.

- The boundary layer on the upper surface thickens more rapidly due to the adverse pressure gradient.

Reasoning: As the flow moves over the upper surface at a 5° angle of attack, the pressure gradually increases in the direction of the flow. This is called an adverse pressure gradient and leads to the thickening of the boundary layer. In this region, the boundary layer is forced to slow down as the pressure rises, causing the boundary layer to grow thicker. If the adverse pressure gradient becomes strong enough, it can cause flow separation, but initially, it results in a thicker boundary layer.

- Minor flow separation is visible near the trailing edge, as indicated by streamline divergence and a small recirculation region.

Reasoning: As the flow moves over the airfoil, the adverse pressure gradient over the upper surface can eventually cause the boundary layer to lose energy and separate from the surface. This results in a small recirculation region or wake at the trailing edge, where the flow direction changes and forms eddies. The streamline divergence indicates this separation region, where the flow no longer follows the contour of the surface, leading to the formation of turbulent wake regions behind the airfoil.

- Streamlines bend more sharply around the leading edge, showing increased flow acceleration over the upper surface.

Reasoning: At an angle of attack, the flow accelerates over the upper surface as it is forced to follow the curvature of the airfoil. The sharp bending of the streamlines around the leading edge indicates an increase in velocity as the flow accelerates. This is a result of the flow being constricted around the leading edge and the subsequent increase in velocity along the upper surface, which contributes to the lower pressure observed on the upper surface. The sharper curvature of the streamlines indicates that the flow is being compressed, which accelerates the fluid over the upper surface.

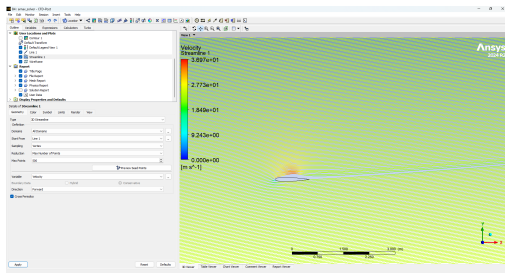


Fig. 18: Streamline contours at 5° angle of attack in ANSYS

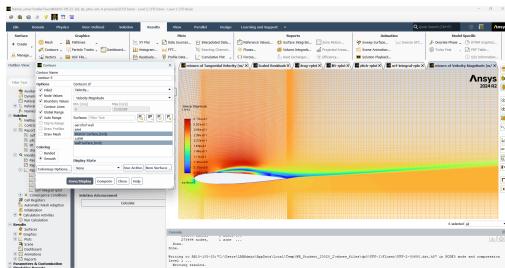


Fig. 19: Velocity contours at 5° angle of attack in ANSYS

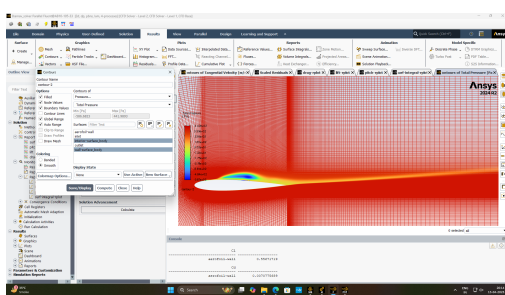


Fig. 20: Pressure contours around the airfoil at 5° angle of attack

Observations:

- At 0° AOA, the flow is symmetric, and there is negligible lift with very low drag.
- At 5° AOA, lift is generated due to pressure difference, and drag increases slightly. Mild flow separation may occur near the trailing edge.

B. Discussion

Theoretical Derivation of Lift and Drag Coefficients:

To analyze the performance of the NACA 0012 airfoil, we consider an incompressible, inviscid, and irrotational flow using thin airfoil theory. For a symmetric airfoil like NACA 0012, the camber line is zero.

a) 1. *Lift Coefficient (C_L)*:: The thin airfoil theory provides the following expression for the lift coefficient:

$$C_L = 2\pi\alpha$$

where:

- α is the angle of attack in radians.

For example:

At $\alpha = 0^\circ = 0 \text{ rad}$,

$$C_L = 2\pi(0) = 0$$

At $\alpha = 5^\circ = \frac{5\pi}{180} \text{ rad} \approx 0.0873 \text{ rad}$,

$$C_L = 2\pi(0.0873) \approx 0.548$$

This linear relationship between C_L and α holds true for small angles (typically $\alpha < 10^\circ$) and matches experimental trends for symmetric airfoils under laminar, attached flow.

b) 2. *Drag Coefficient (C_D)*:: For inviscid flow, drag is theoretically zero due to D'Alembert's paradox. However, in real flow with viscosity, drag appears due to flow separation and wake formation. As the angle of attack increases, the pressure difference between the front and rear of the airfoil increases, resulting in a larger wake and thus higher drag.

c) 3. *Lift-to-Drag Ratio (L/D)*::

$$\frac{L}{D} = \frac{C_L}{C_D}$$

At low angles, L/D is high due to low drag. As α increases, drag increases faster than lift, reducing L/D .

Physical Interpretation and Comparison with Simulation Results: From the simulation:

- At 0°, the pressure distribution is symmetric across the upper and lower surfaces, leading to zero or negligible lift.
- At 5°, the upper surface experiences a lower pressure while the lower surface sees a higher pressure, producing net lift, as expected from Bernoulli's principle.
- The pressure contours and streamlines show increased curvature and flow acceleration over the upper surface at 5°, consistent with thin airfoil theory.
- Velocity contours confirm higher velocities over the upper surface, matching the predicted pressure drop (via Bernoulli's equation).
- Drag increases due to formation of a longer wake and slight flow separation, which is evident in the streamline and pressure plots.

Thus, the simulation results are consistent with theoretical predictions in terms of:

- Linear increase of C_L with α
- Symmetric flow at 0°
- Increasing drag with increasing angle due to wake formation

Comparison of Theoretical and Simulated Coefficients: The following table presents a comparison between the theoretical and CFD-obtained values of the lift and drag coefficients at two angles of attack:

TABLE III: Comparison of Lift and Drag Coefficients

Angle of Attack	Method	C_L	C_D
0°	Theoretical	0.000	≈ 0 (ideal)
	CFD Simulation	0.02	0.0066
5°	Theoretical	0.548	—
	CFD Simulation	0.52	0.0071

VIII. CONCLUSION

Possible Reasons for Deviation in Results

The slight deviation between the theoretical and simulated lift and drag coefficients can be attributed to several factors, including:

- **Viscous Effects:**

- Theoretical calculations assume inviscid (no viscosity) flow, while CFD simulations account for viscous effects, which contribute to drag and boundary layer formation. This leads to higher drag in the simulation compared to the ideal theoretical case.

- **Reynolds Number Effects:**

- The Reynolds number in the CFD simulation might not exactly match the conditions assumed in the theoretical analysis. Differences in flow characteristics such as boundary layer thickness and flow separation could lead to variations in the lift and drag coefficients.

- **Mesh Resolution:**

- The accuracy of the CFD simulation heavily depends on the mesh resolution, especially near the airfoil surface. A coarser mesh could result in less accurate predictions of the boundary layer and flow separation, affecting the lift and drag results.

- **Flow Separation and Wake Effects:**

- At higher angles of attack (e.g., 5°), flow separation and wake formation become more significant. The thin airfoil theory does not account for these effects, which could cause the drag in the simulation to be higher than the theoretical prediction.

- **Turbulence Modeling:**

- The theoretical lift coefficient is derived under the assumption of steady, laminar flow. In contrast, the CFD simulation may incorporate turbulence models, especially near the airfoil surface, which may lead to slight discrepancies in the results.

- **Boundary Condition Assumptions:**

- The theoretical model assumes ideal boundary conditions, such as an infinite flow field and perfect symmetry. In practice, finite computational domains, wall effects, and discretization can cause minor deviations from the expected results.

- **Angle of Attack Adjustment:**

- In CFD simulations, small adjustments or uncertainties in the precise angle of attack (i.e., due to meshing or setup) could slightly affect the lift and drag

calculations, causing a deviation from the theoretical values.

- **Numerical Approximation:**

- The CFD solver employs numerical methods to solve the governing equations, which inherently involves approximations. These approximations can introduce slight differences in the predicted values compared to the ideal theoretical analysis.

The CFD simulations on the NACA 0012 airfoil provide insight into the aerodynamic performance at low angles of attack. The results are in good agreement with literature values and reflect expected trends. Further accuracy can be achieved by increasing the number of iterations and considering turbulent flow effects.

REFERENCES

REFERENCES

- [1] Anderson, J. D., *Fundamentals of Aerodynamics*, 5th ed., New York: McGraw-Hill, 2010.
- [2] White, F. M., *Fluid Mechanics*, 7th ed., New York: McGraw-Hill, 2011.
- [3] Cebeci, T. and Bradshaw, P., *Momentum Transfer in Boundary Layers*, Hemisphere Publishing, 1988.
- [4] NASA Langley Research Center, *NACA 0012 Airfoil Validation*, 2007. Retrieved from https://turbmodels.larc.nasa.gov/naca0012_val.html.